Effect of the water saturation of aggregates on the shrinkage induced cracking risk of concrete at early age

Rachid Cortas, Emmanuel Rozière, Stéphanie Staquet, Ameur Hamami, Ahmed Loukili, Marie-Paule Delplancke-Ogletree

▶ **To cite this version:**

Rachid Cortas, Emmanuel Rozière, Stéphanie Staquet, Ameur Hamami, Ahmed Loukili, et al.. Effect of the water saturation of aggregates on the shrinkage induced cracking risk of concrete at early age. Cement and Concrete Composites, 2014, 50, pp.1-9. ⟨10.1016/j.cemconcomp.2014.02.006⟩. ⟨hal-02076360⟩

HAL Id: hal-02076360

https://hal.science/hal-02076360v1

Submitted on 30 Dec 2025

HAL is a multi-disciplinary open access archive for the deposit and dissemination of scientific research documents, whether they are published or not. The documents may come from teaching and research institutions in France or abroad, or from public or private research centers.

L'archive ouverte pluridisciplinaire **HAL**, est destinée au dépôt et à la diffusion de documents scientifiques de niveau recherche, publiés ou non, émanant des établissements d'enseignement et de recherche français ou étrangers, des laboratoires publics ou privés.

Distributed under a Creative Commons CC BY-NC 4.0 - Attribution - Non-commercial use - International License

Effect of the water saturation of aggregates on the shrinkage induced cracking risk of concrete at early age

R. Cortas [a,b], E. Rozière [a], S. Staquet [b], A. Hamami [b], A. Loukili [a,*], M.-P. Delplancke-Ogletree [c]

[a] L'UNAM Université, Institut de Recherche en Génie Civil et Mécanique, GeM-UMR CNRS 6183, Centrale Nantes, 1 rue de la Noe, BP 92101, F-44321 Nantes Cedex 3, France

[b] Service BATir, Université Libre de Bruxelles, Brussels, Belgium

[c] Service 4MAT, Université Libre de Bruxelles, Brussels, Belgium

This work consists in studying the effect of the water saturation of aggregates on the development of shrinkage and the potential cracking risk of early age ordinary concrete. Different concretes were obtained from a given concrete mixture by changing only the initial degree of saturation of limestone aggregates. Three degrees of saturation were studied, namely: 0% (dry aggregates), 50% (partially saturated aggregates) and 100% (saturated aggregates). From the experimental results, the early age behaviour and the mechan ical properties of the concrete strongly depend on the water saturation of aggregates. A relative cracking risk was estimated from a stress based approach and experimentally assessed parameters. The potential risk of cracking of these different concretes was shown to be different. Even if the total water content is kept constant, the water remaining in the cement paste actually depends on the initial water saturation of aggregates. The early age behaviour of concrete and the development of its early age properties depend on the amount of added water during the mixing.

1. Introduction

Plastic shrinkage cracking is often observed on slabs, slabs on grade, and raft slab foundations. The starting point of this study was a site investigation. Cracking across a 20 cm thick raft slab foundation was observed during the first 24 h after casting. The distribution and the direction of the cracks showed that they were not due differential settlement or bending. The concrete mixture and curing complied with standard requirements. The target Effective water/Cement (W_{eff}/C) ratio was 0.42. The Effective water content used in the mix design of concrete is the total water content (mixing water + water supplied by aggregates + water pro vided by chemical admixtures) from which the water absorbed by the aggregates is subtracted. The mixture proportions were ana lysed from the data provided by the ready mix concrete supplier. The water saturation of aggregate was relatively high thus the Added water/Cement ratio (0.34) was significantly lower than the target Effective water/Cement ratio (0.42). The lower the water/cement ratio, the higher the plastic shrinkage strain and early age cracking risk. This example confirms that the water saturation of aggregates is an influencing parameter to understand the cracking risk of concrete subjected to restrained shrinkage.

Plastic shrinkage refers to shrinkage occuring during the setting and early hardening of concrete. It is due to external drying and self dessiccation caused by the hydration of cement. External drying can be avoided by a good curing of concrete at early age, thus this study mainly deals with autogenous shrinkage. When shrinkage is restrained, the concrete is subjected to tensile stresses that are likely to cause cracking. The concrete cracking phenomena depend on the magnitude and kinetics of shrinkage, the evolution of the mechanical properties of the concrete (elastic modulus and tensile strength), and creep. Creep is significant at early age. However early age creep and relaxation magnitudes are difficult to assess unless sophisticated testing is used.

It should be mentioned that the aggregates form 70% of the concrete total volume. Even if aggregates are usually considered as inert material, their properties influence the shrinkage of con crete. Aggregate restrains the shrinkage of hardened cement paste, thus the modulus of elasticity is an influencing property. Aggregate is a porous material and it is likely to shrink or swell [1]. The poros ity and pore size distribution influences the water saturation and the capillary tension. How could the supplied or absorbed water be taken into account? The *Effective water* concept is approximate because it does not take into consideration the actual aggregates

* Corresponding author. Tel.: +33 2 40 37 16 67; fax: +33 2 40 37 25 35.
E-mail address: ahmed.loukili@ec-nantes.fr (A. Loukili).

Accepted manuscript

absorption kinetics. The actual amount of water absorbed by the aggregates can be different from the theoretical amount, which is based on absorption capacity of the aggregates. As a result, the actual paste porosity is quite different from the corresponding the oretical one and particularly in the zones surrounding aggregates, where an interfacial transition zone is likely to appear between the paste and the aggregates [2]. Aggregates have a significant influence on the shrinkage, strength, and other concrete properties [1,3,4], and consequently on the concrete cracking.

The effect of lightweight aggregate saturation on the concrete shrinkage has already been investigated in literature [5 8]. These researchers have proposed the use of saturated lightweight aggre gates to provide "internal" curing for the concrete and mitigate autogenous shrinkage. Few studies deal with the influence of water saturation of natural aggregates on early age shrinkage [9]. The porosity of aggregates is generally expressed in terms of 24 h water absorption (WA_{24}). Water absorption usually ranges from 0.5% to 2%. But the availability of natural aggregate for concrete is becoming a crucial question. As a consequence concrete produc ers must use locally available resources even if aggregates show higher water absorption. Limestone aggregates constitute 25% of aggregates used in France for concrete production. Their water absorption usually ranges from 0.5% to 4%. Alhozaimy [10] have shown that dry limestone aggregates did not fully absorb the part of added water required to compensate the aggregates absorption, and thus, lead to an increase of the actual (W/C) ratio of the mixes increasing the initial slump and decreasing the compressive strength. Pereira et al. [11] concluded that wet aggregates will not absorb water from the cement paste contributing to a dense cement aggregate interface whereas dry aggregates absorb water contributing to a porous cement aggregate interface zone. Some studies suggest improved interfacial properties when water and cement based materials are drawn into the porous aggregate. The absorption of water by the partially saturated lightweight aggregate results in a thinner interfacial transition zone (ITZ) than in normal aggregate mortar and a denser paste between 10 and 50 μm from the surface of the lightweight aggregate [12]. More over lightweight aggregate such as pumice affects the morphologic properties of ITZ [13]. The results are consistent with studies about the interface between repair mortars and concrete substrates. Courard et al. [14] have shown that the saturation levels of sub strate concrete higher than 50% and lower than 90% are requested to a better bonding of repair mortars. Mallat and Alliche [15] have also shown that saturated concrete substrate with a dry surface can be considered as the best solution and gives the highest bond strengths compared to the other moisture conditions.

This paper presents a comprehensive experimental study on the effect of the water saturation of limestone aggregates on the shrinkage induced cracking risk of concrete at early age. The water absorption of the limestone aggregate used in this study (3.2%) is relatively high, but the limestone aggregate complies with the specifications of the standards on aggregate for concrete and it is ordinarily used as aggregate. The investigation was carried out un der sealed and drying conditions. The cracking analysis is based on autogenous shrinkage strains and elastic stress/strength approach. The results obtained for concrete mixtures with different satura tion degrees of aggregates (0%, 50%, and 100%) are presented, ana lysed and discussed in this paper to demonstrate the prevailing effect of the (Added water/Cement) ratio.

2. Materials and concrete mixtures

2.1. Materials

Limestone crushed gravel (0/22.4 mm) was specially chosen for this study due to their relatively high porosity. The water absorption coefficient (WA_{24}) of gravel was 3.2% (in percentage of dry mass after water immersion during 24 h) according to EN 1097 6 standard [16]. In other words, it represents 7.9% in volume. A sea sand (S1 0/4) and a crushed dense limestone sand (S2 0/4) were used in all the mixtures tested in our study (Table 1). CEMI 52.5 N Portland cement was also used (Table 2). The materials compositions and properties are given in Table 3. The defloccula tion of particles was ensured thanks to a polycarbolaxate type superplasticizer (Sp). The mixtures were made with tap water.

2.2. Mixtures

The reference mixture remains the same; the only variable is the initial water saturation of gravel. The three studied concretes are named S0%, S50% and S100% respectively for that containing dry, partially saturated and totally saturated gravel. The saturation degree of sand remains constant in the three mixtures. The con cretes mixtures compositions are given in Table 3.

The water saturation of gravel is assessed from the mass water content and the absorption coefficient, in percent (Eq. (1)). Added water (Eqs. (2) and (3)) was adjusted to maintain the effective water constant (Eq. (4)) by considering the gravel water content. The superplasticizer content varied to obtain the same workability (slump).

$$S \quad \frac{W_{\text{Gravel}}}{WA_{24}} \times 100 \tag{1}$$

where S is the saturation (%), W_{Gravel}. is the water content of gravel (%), and WA_{24} is the water absorption (%).

$$W_{\text{added}} \quad W_{\text{eff.}} + W_{\text{absorption}} \quad W_{\text{aggregates}} \quad W_{\text{superplasticizer}} \tag{2}$$

$$W_{\text{total}} \quad W_{aggregates} + W_{\text{added}} \tag{3}$$

$$W_{\text{aggregates}} \quad W_{\text{gravel}} + W_{\text{sand}} \tag{4}$$

where

W_{added} is water actually added in the mixture.
W_{eff} is the effective water content.
$W_{\text{absorption}}$ is the water theoretically absorbed by dry aggregates (gravel and sand).
$W_{\text{aggregates}}$ is the aggregates water content (gravel and sand).
$W_{\text{superplasticizer}}$ is the water part of superplasticizer.
W_{total} is the water added in the mixture containing dry aggregates.

3. Experimental methods

3.1. Plastic shrinkage and setting time measurement

The development of plastic shrinkage was measured using a prism shaped steel mould device ($70 \times 70 \times 280\ \text{mm}^3$) covered with Polytetrafluoroethylene (PTFE) to limit the friction between the concrete and the mould [17]. The concrete was poured into an envelope built using two PVC plates ($70 \times 68 \times 5\ \text{mm}^3$) also used as reflecting plates and a plastic sheet (Fig. 1). The concrete specimen is cast in the steel mould. The ends of the mould are perforated to ensure a circular opening which enables monitoring the movement of the reflecting plates anchored to the ends of the sample using two laser sensors. The accuracy of the laser sensors is 2 μm. The temperature of concrete is controlled using water circu lation in both the side walls and the steel mould bottom (Fig. 1). As a result, the concrete samples are stored in isothermal conditions. The actual concrete temperature is monitored using a thermocou ple placed in the center of the sample. Previous studies [18] showed that the maximum temperature increase in concrete did not exceed 1 °C. In this study tests were performed at 20 °C and

Manuscript

Table 1
Properties of aggregates.

	Sea sand (0/4 mm)	Limestone sand (0/4 mm)	Crushed gravel (4/22.4)
Mineralogy	Mixed	Dense limestone	Porous limestone
Water absorption WA_{24} (%)	0.60	0.77	3.20
Bulk density	2.58	2.65	2.46
Apparent (skeletal) density			2.68

Table 2
Properties of cement.

	CEM I 52.5
Clinker (%)	96
C_3S (%)	58
C_2S (%)	10
C_3A (%)	12
C_4AF (%)	8
$CaCO_3$ (%)	4
Blaine fineness (m^2/kg)	368

Table 3
Composition and properties of concrete mixtures (kg/m^3). (a) Theoretical mixtures composed by dry aggregates. (b) Real mixtures.

	S0%		S50%		S100%	
	a	b	a	b	a	b
Gravel (kg/m^3)	1000	1000	1000	1016	1000	1032
Sea sand (kg/m^3)	367	378	367	378	367	378
Limestone sand (kg/m^3)	377	389	377	389	377	389
Cement, C (kg/m^3)	350		350		350	
Superplasticizer (Sp) (kg/m^3)	1.0		1.25		1.5	
W_{eff} Eq. (2)	175		175		175	
W_{Sp}	0.8		1		1.2	
W_{total} Eq. (3)	211		211		211	
W_{sand} Eq. (4)	0	23	0	23	0	23
W_{gravel} Eq (4)	0	0	0	16	0	32
W_{added} Eq. (2)	211	188	211	172	211	156
W_{eff}/C	0.50		0.50		0.50	
W_{added}/C	0.54		0.49		0.44	
Aggregates/sand	1.34		1.34		1.34	
Paste volume (L/m^3)	288		288		288	
Sp/C (%)	0.29		0.36		0.43	
Slump (mm)	160		180		170	
Compressive strength						
$f_{C,\ 1d}$ (MPa)	15.5		20.5		17.0	
$f_{C,\ 2d}$ (MPa)	22.6		31.4		26.9	
$f_{C,\ 28d}$ (MPa)	42.6		50		47.5	

50% RH. The tests started about 20 30 min after the first contact between water and cement.

The setting time measurement was determined by Vicat test according to the standard EN 196 3 standard [19]. The test was carried out on mortars obtained from concrete using a 5 mm sieve. The monitoring of the setting was done using an automatic device. The specimens were placed in temperature controlled water at 20 °C to prevent the mortar from drying and to ensure a constant temperature during the test.

3.2. Early age autogenous deformation measurement

The autogenous deformation measurements of the studied con cretes were carried using a BTJADE device [20,21]. This latter is composed by a corrugated PVC mould [22] with a stiffness assumed to be negligible. As shown in Fig. 2, a thermocouple is inserted into the concrete specimen. The effective height of the concrete sample (L_0 = 250 mm) is the reference length for calculat ing the autogenous shrinkage. The sample and the mould are main tained vertically by means of a metal frame. The deformation of the sample is measured by means of an external displacement sensor. The device is completely immersed inside a temperature con trolled bath and totally surrounded by water to insure isothermal conditions. More detailed information on this device can be found in [21].

The specimen autogenous deformations are obtained from the recorded data (displacement and temperature) after correction with the thermal variations [23]. The specimen thermal deforma tion is computed by assuming a constant specimen thermal expan sion coefficient after setting [24]. It was determined on basis of temperature cycles at the end of the test. In order to verify the repeatability of measurements, this test was carried out on 3 spec imens, and the results given in Fig. 6 are the average deformation curve. Note that the BTJADE device [20] is characterised by a very limited uncertainty to 6 μm/m for the measurement of the total deformation (without thermal corrections) and to 8 μm/m for the measurement of the autogenous shrinkage for this type of con crete. Therefore the BTJADE remains a good autogenous shrinkage device measurement for low values (i.e. up to a maximum of 50 (μm/m) at the age of 24 h) and detecting a low relative differ ence between compositions. The initial setting time determined by Vicat test was taken as time zero. Before setting the shrinkage is mainly due to chemical shrinkage and it does not induce stresses. Moreover as the mould of BTJADE device has a negligible stiffness thus the deformation before setting corresponds to the settlement of the concrete sample.

3.3. Evolution of the elastic properties at early age

The FreshCon system (Fig. 3) which was developed at the Uni versity of Stuttgart [25] was used herein to monitor the evolution of the elastic properties of concrete at early age using ultrasonic *p* and *s* waves. It consists in a specific mold (for concrete or mortar) equipped with two piezoelectric transducers (one transmitter and one receiver). A computer equipped with a data acquisition card is linked to a piezoelectric high voltage pulser to generate a high voltage short rectangular wave (typically 800 V with a pulse width

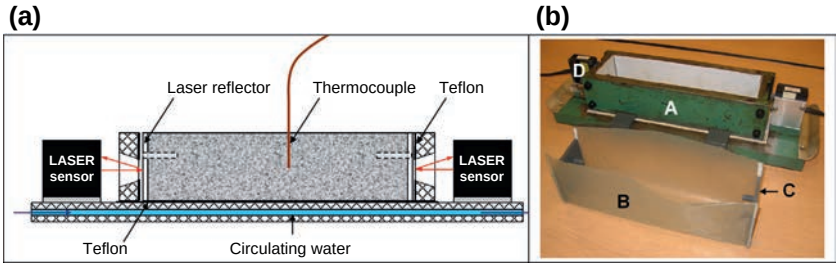

Fig. 1. Plastic shrinkage testing. (a) Plastic shrinkage measuring device and (b) plastic shrinkage mould, A. mould, B. plastic sheet, C. Laser reflector (PVC), D. laser sensor.

Accepted Manuscript

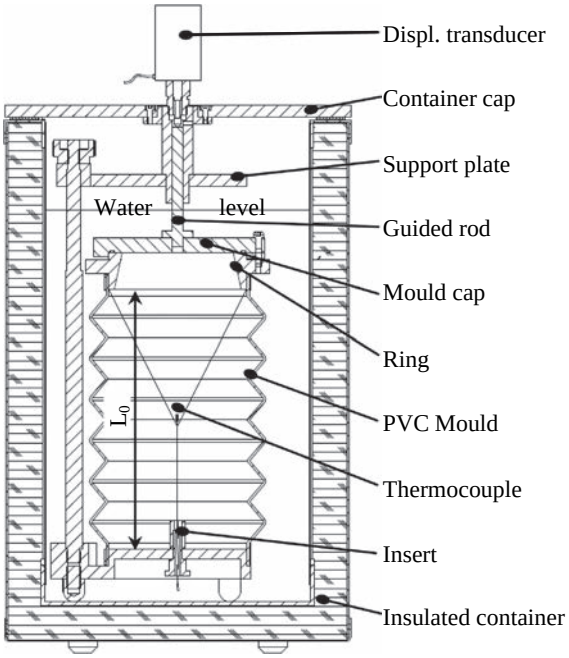

Fig. 2. Autogenous shrinkage test rig.

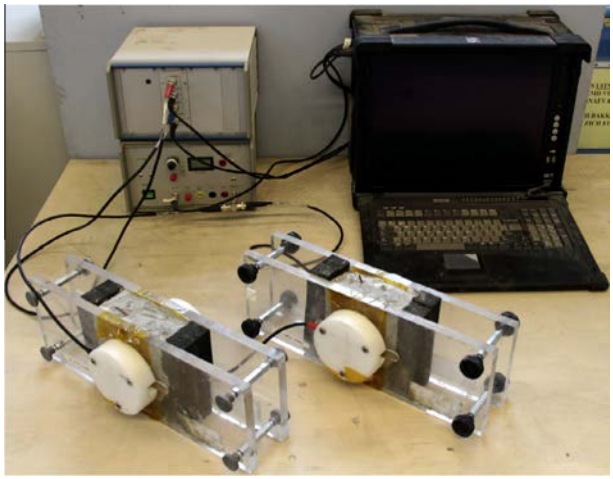

Fig. 3. Ultrasonic monitoring device. (a) Computer with DAQ card, (b) amplifier, (c) piezoelectric sensor, (d) container, (e) preamplifier.

between 2.5 and 5 μs). A wide band ultrasonic (mechanical) wave is generated and picked up by the receiver of which the signal is amplified after traveling through the material. The software in the computer automatically computes the time it takes for the wave to travel from the transmitter to the receiver and deduces the velocity of the wave. More detailed information on this device can be found in [26]. The test was carried out in an air conditioned room at 20 °C and that the concrete sample was protected from desiccation by the use of a plastic foil.

The evolution of the dynamic Poisson ratio υ_{dyn} and the dynamic elastic modulus E_{dyn} is obtained using the ultrasonic device. Their values are obtained as a function of the compression (p) and shear (s) wave velocities using Eqs. (5) and (6) which are only valid for linear elastic, isotropic media [27]:

$$v_{dyn} \quad \frac{\frac{1}{2}\cdot v_p^2 \quad v_s^2}{v_p^2 \quad v_s^2} \tag{5}$$

$$E_{dyn} \quad v_p^2 \cdot \rho_c \cdot \frac{(1+v_{dyn})\cdot(1 \quad 2v_{dyn})}{1 \quad v_{dyn}} \tag{6}$$

where ρ_c is the density, v_p is the P wave velocity and v_s the S wave velocity. P waves and S waves were simultaneously measured on the same concrete with dedicated FreshCon molds.

3.4. Porosity and pore size distribution

The porosity and pore size distribution were determined from mercury intrusion porosimetry (MIP) on one sample of about 1 cm^3. The samples were dried at 20 °C and 50% RH for 24 h before the test. (MIP) was carried out with a Micromeritics Porosimeter (Autopore IV 9500). The range of pressure reached 400 MPa. This pressure range allows the mercury to penetrate pores ranging between 0.003 μm and 360 μm diameter, according to Laplace law. However, such a technique only allows the estimation of the inlet pore diameter [28].

3.5. Evolution of the hydration degree at early age

The degree of hydration and the free water content of the studied materials were obtained by using a Thermo Gravimetric Analysis (TGA). The experiments were performed on cement pastes obtained from crushed concrete by sieving at different ages: 3, 6, 9 and 24 h. Before sieving, the materials were kept in sealed condi tions at 20 °C. The TGA was carried out under inert atmosphere (helium) over a temperature range 25 1000 °C with a heating rate of 20 °C/min. This experiment allows obtaining the amount of free

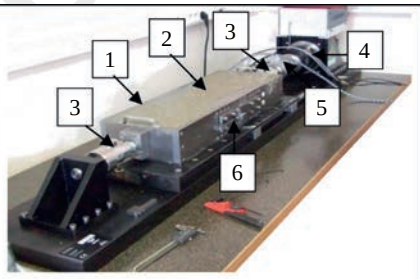

(a)

1: Steel mould, 2: Concrete specimen, 3: Spherical pin connection, 4: Electric actuator, 5: Load cell, 6: LVDT2

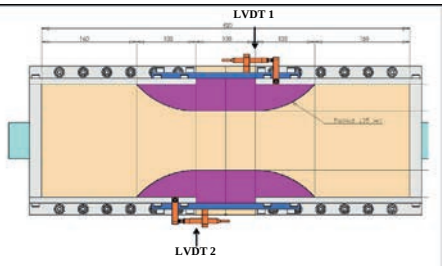

(b)

Top view of the steel mould.

Fig. 4. Tensile testing machine.

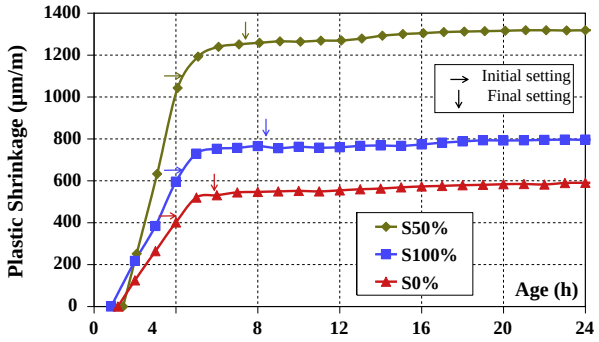

Fig. 5. Evolution of the plastic shrinkage for the three mixtures.

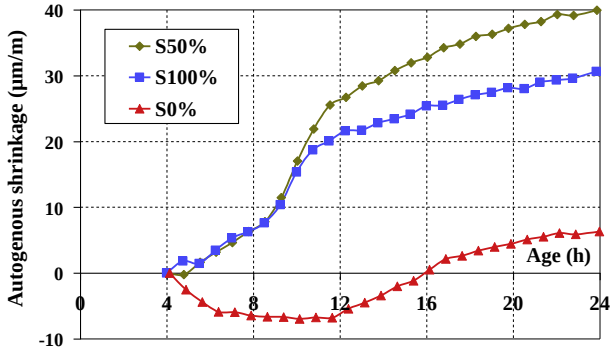

Fig. 6. Effect of aggregate moisture content on the evolution of autogenous shrinkage from the time of initial setting.

water from the mass loss between 25 °C and 150 °C [29]. The amount of chemically bounded water was obtained from the mass loss between 150 °C and 600 °C. The degree of hydration α (%) was calculated by using Eq. (7) [29]:

$$\alpha\ (\%) \quad \frac{w\ (t)}{w\ (\infty)} \times 100 \tag{7}$$

where $w\ (t)$ (%) is the amount of chemically bounded water at the age t of the material, $w\ (\infty)$ (%) is the amount of chemically bounded water for a total hydration of the cement contained in the material. $w\ (\infty)$ is usually calculated from the chemical composition of the cement using the Bogue formula [30].

3.6. Tensile strength of early age concrete

The assessment of the tensile strength of early age concrete is necessary to understand the cracking due to restrained shrinkage. New direct tensile testing apparatus and experimental procedure were designed to provide reliable data on concrete specimens at early age. Fig. 4 shows the tensile testing machine. The load is applied horizontally by an electric displacement controlled actuator. The load cell is placed between the actuator and the mobile part of the mould [31]. The dogbone shaped mould actually comprises two halves with curved transitions to a central part with reduced constant section, 100 mm high, 100 mm long, and 105 mm wide. The inner face of the mould is covered with PTFE and protected with thin polyethylene sheets during the test. The two parts of the mould are linked to the frame and the load cell by spherical pin connections. The stress was deduced from the measured load and the cross section (100×105 mm^2).

The concrete specimen was cast in the steel mould just after mixing then vibrated in one layer. An external frame was placed on the plate to avoid displacements of the two halves of the mould due to the vibration and pressure of fresh concrete. The specimen was covered until testing with a polyethylene sheet to avoid drying. The ambient temperature was 20 °C. The loading rate of the actuator was 5 µm per second.

4. Experimental results and discussion

4.1. Early age behaviour

4.1.1. Plastic shrinkage and setting time

The plastic shrinkage of the three concretes showed significant differences. The magnitude at 24 h ranged from 600 to 1300 µm/m (Fig. 5). (S 50%) showed the highest plastic shrinkage and (S 0%) the lowest values. The mixture (S 0%) contained more added water because it was made of dry aggregates. The higher the (W_{added}/C) ratio, the higher the bleeding rate [32] thus the concrete (S 0%) was likely to draw benefits from bleeding water on the surface which mitigated the plastic shrinkage. (S 50%) had the largest plastic shrinkage because it did not draw benefit from the bleeding water as in the case of (S 0%) and from the internal curing of saturated aggregates as in the case of (S 100%). As shown in Fig. 5, final setting occurred earlier for (S 0%) than (S 50%) and (S 100%). Setting time was indirectly related to the actual quantity of added water in each composition. The lower the added water, the higher the superplasticizer content and the later the setting, as superplasticizers generally delay the setting of cement pastes. (S 100%) was characterised by the lowest added water and as a consequence the last final setting time.

4.1.2. Autogenous deformation

Even though the autogenous shrinkage of the concrete with a (W_{eff}/C) equal to 0.5 is relatively low, it could be measured. Autogenous shrinkage is due the hydration of cement thus it cannot be completely avoided, whereas concrete can be prevented from drying (by curing compounds or water) to reduce the plastic shrinkage magnitude. Thus the purpose was to understand to what extent autogenous shrinkage was involved in cracking. As shown in Fig. 6, the autogenous deformations relatively change with respect to the variation of gravel saturation. These amplitudes are very low compared to those obtained when monitoring the plastic shrinkage. However the same trends and ranking can be observed. The concrete mixture containing dry aggregates (S 0%) exhibited a swelling phase during the first 12 h which was absent in the case of saturated (S 100%) and intermediate concrete (S 50%). The cement paste of the concrete with dry aggregates (S 0%) contained more added water than the paste of the two other concretes (S 50%) and (S 100%). Experimental studies showed that concrete mixtures with high (W_{added}/C) are likely to show swelling during the autogenous shrinkage test [33]. The influence of bleeding water on the measurement of autogenous deformations has been studied [34,35]. Bleeding of concrete mainly results from the self weight consolidation of the granular skeleton [36]. The higher the (W_{added}/C) the higher bleed water is observed. The bleed water is likely to compensate the effects of self desiccation when reabsorbed, and cause swelling.

The concrete made of saturated aggregates (S 100%) contained less water in the paste and thus it showed higher autogenous shrinkage than the concrete made of dry aggregates (S 0%). The intermediate concrete (S 50%) showed the highest autogenous shrinkage. This can be explained by the fact that the cement paste of the intermediate concrete (i) contained less water than the dry concrete (S 0%) and, (ii) drew less benefit from the internal curing of saturated aggregates compared to the concrete made of

Accepted Manuscript

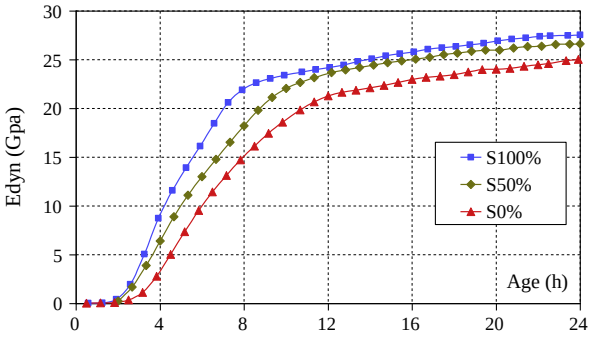

Fig. 7. Effect of aggregate moisture content on the evolution of dynamic modulus at early age.

saturated aggregates (S 100%). As a conclusion, the intermediate concrete (S 50%) was the most sensitive to autogenous shrinkage.

4.1.3. Evolution of dynamic Young's modulus

Fig. 7 shows the evolution of the dynamic Young's modulus as a function of the age of concrete. This dynamic elastic modulus was slightly larger in the case of (S 50%) and (S 100%) compared to (S 0%). This is because a smaller quantity of added water was used in theses mixtures which lead to lower actual (W/C) ratios and higher strengths (thus a larger dynamic elastic modulus). It should be noticed here that at the age of 6 h the difference of modulus between (S 0%) and the S (100%) was 70% whereas at the age of 24 h the difference was only 10%.

4.2. Microstructural characterization

4.2.1. Porous network properties

Mercury Intrusion Porosimetry (MIP) was performed on concrete and cement pastes obtained from crushed concrete by sieving at different ages: 3, 6, 9 and 24 h. MIP analyses provided main pore diameters. The main pore diameter was determined from the differential intrusion vs. pore diameter curve. The peak observed on the curve is the diameter corresponding to the maximum intrusion. The main pore diameter is plotted as a function of the age of concrete in Fig. 8 and the cumulative intrusion of mercury is plotted as a function of pore diameter in Fig. 9.

The main pore diameter of concrete decreased as a consequence of the hydration of cement. It was strongly influenced by the properties of the cement paste. At 6 and 9 h, the main pore diameter of the concrete made of dry aggregates (S 0%) was significantly higher than the main pore diameter of concretes S 50% and S 0%. The Added water/Cement ratio increased with a decrease of the initial water saturation of aggregates, which caused an increase of the main pore diameter of hardening cement paste.

According to Fig. 9a, the cumulative porosity was different depending on the water saturation of aggregates for the same theoretical concrete mixture. Fig. 9.b presents the distribution of porosity for each concrete at the age of 24 h:

1st Phase: microporosity, pore diameters smaller than 0.1 μm.
2nd Phase: mesoporosity, pore diameters between 0.1 and 0.4 μm.
3rd Phase: macroporosity, pore diameters greater than 0.4 μm.

The microporosity (1) represents the porosity of hydration products [37], it was approximately the same for the three concretes. Microporosity is directly related to the degree of hydration of cement. The mesoporosity (2) represents the intermediate porosity of concrete, it depended on the initial degree of saturation of aggregates. The macroporosity (3) is influenced by the quantity of added water in concrete [38]. (S 0%) showed the highest macroporosity because it had the highest added water content in the paste. According to Table 3, it should be noticed that (S 100%) had a higher long term compressive strength (Age > 24 h) than concrete made of dry aggregates (S 0%) and this observation is consistent with the difference of the macroporosity. (S 50%) showed the same micro and macroporosity as (S 100%) but lower mesoporosity. This is consistent with higher strength. It can be explained by the following assumptions (i) it contained less added water than the concrete (S 0%), (ii) and the lower mesoporosity could be due to a less developed interfacial transition zone [2,39] compared to the concrete (S 100%) (This should be verified). It is important to note that the trends and the classification of the compressive strength are the same as for plastic and early age autogenous shrinkage. The concrete (S 50%) containing partially saturated aggregates showed the highest compressive strength, plastic shrinkage, and autogenous shrinkage magnitudes, whereas the concrete (S 0%) containing dry aggregates showed the lowest values.

4.2.2. Hydration evolution

As shown in Fig. 10, the three concrete mixtures had the same evolution of the hydration degree during the first 24 h. The hydration degree is directly related to chemically bounded water which is relatively the same for the three compositions the first 24 h. Hydration degree can be correlated to the microporosity (Fig. 9). The microporosity is actually related to the progress of the reaction of hydration of cement because it represents the porosity of hydration products which was the same for the three compositions.

4.3. Early age cracking risk of concrete

A comprehensive assessment of the cracking risk should not only take into account the stress inducing phenomena, i.e. shrinkage and increase of elastic modulus, but also the beneficial effects of creep or relaxation. The analysis is generally made using

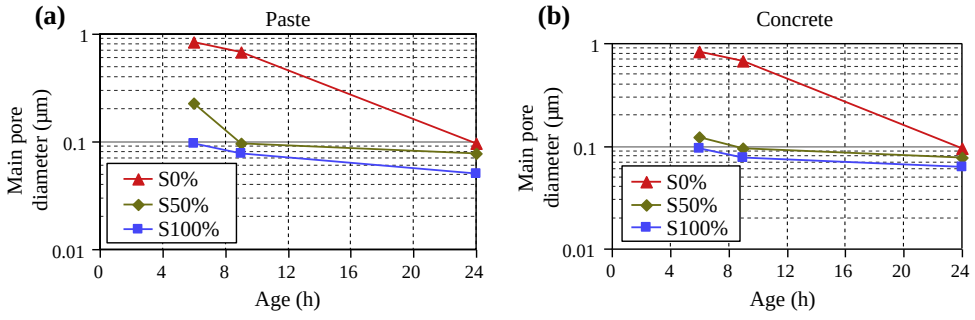

Fig. 8. Main pore diameter of paste (a) and concrete (b).

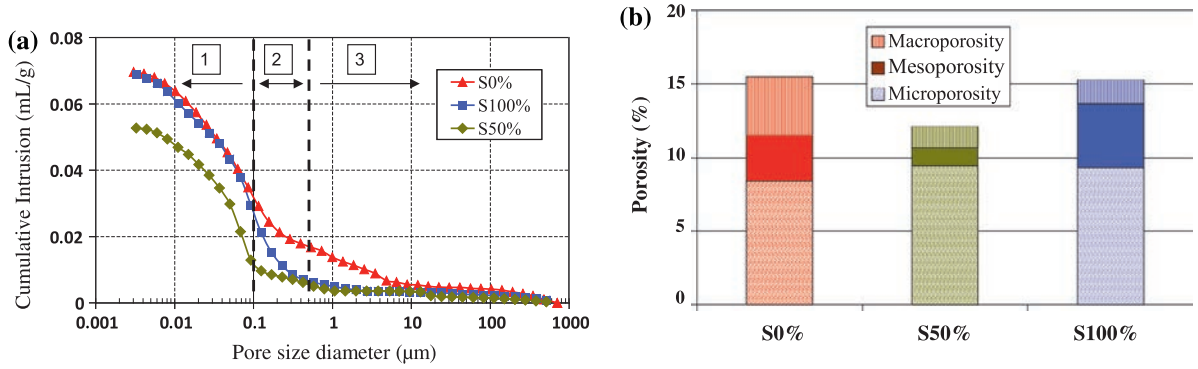

Fig. 9. (a) Cumulative porosity for the three concretes at age of 24 h. (b) Porosity of the three concretes at age of 24 h.

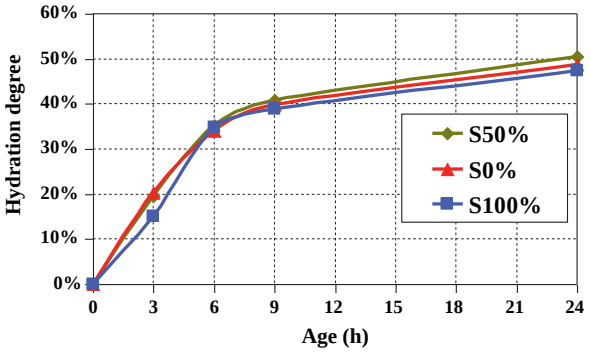

Fig. 10. Evolution of the hydration degree at early age of the three compositions.

restrained shrinkage tests, such as *Temperature Stress Testing Ma chine* (*TSTM*) [40,41]. Autogenous or plastic shrinkage is fully re strained and one can measure the stress generation, the elastic modulus, and relaxation. However the evolution of each parameter is the result of opposite and coupled effects, thus it is difficult to analyse the effects of concrete mixture proportions on each param eter involved in shrinkage cracking [42]. For realistic conditions including thermal and drying effects, tests like TSTM would be appropriate because in this case the goal of the study would be to keep all the coupled effects simultaneously.

An uncoupled approach was applied here, as the objective of the study was to investigate the effect of aggregate moisture content on the shrinkage and cracking of early age concrete, focusing on autogenous shrinkage. The cracking risk assessment from stress/ strength is more reliable than using strain/stress capacity [40,43]. From the early age properties, the developed internal elastic stres ses in the concrete were calculated using the elastic model (Eq. (8)). The dynamic modulus evolution and the autogenous shrink age were both determined previously. The obtained values of the developed internal stresses provide data about the potential crack ing risk of these compositions due to autogenous shrinkage by comparing the internal stresses to concrete tensile strength [41].

$$\sigma(t) \quad \varepsilon(t) \cdot E(t) \tag{8}$$

with:

$\sigma(t)$: Evolution of the estimated internal stresses.

$\varepsilon(t)$: Autogenous shrinkage measured by BTJADE.

$E(t)$: Evolution of the modulus of elasticity measured by FreshCon.

Concrete tensile strength was experimentally assessed at 3, 5, 10, 15, and 24 h using direct tensile test (3.4).

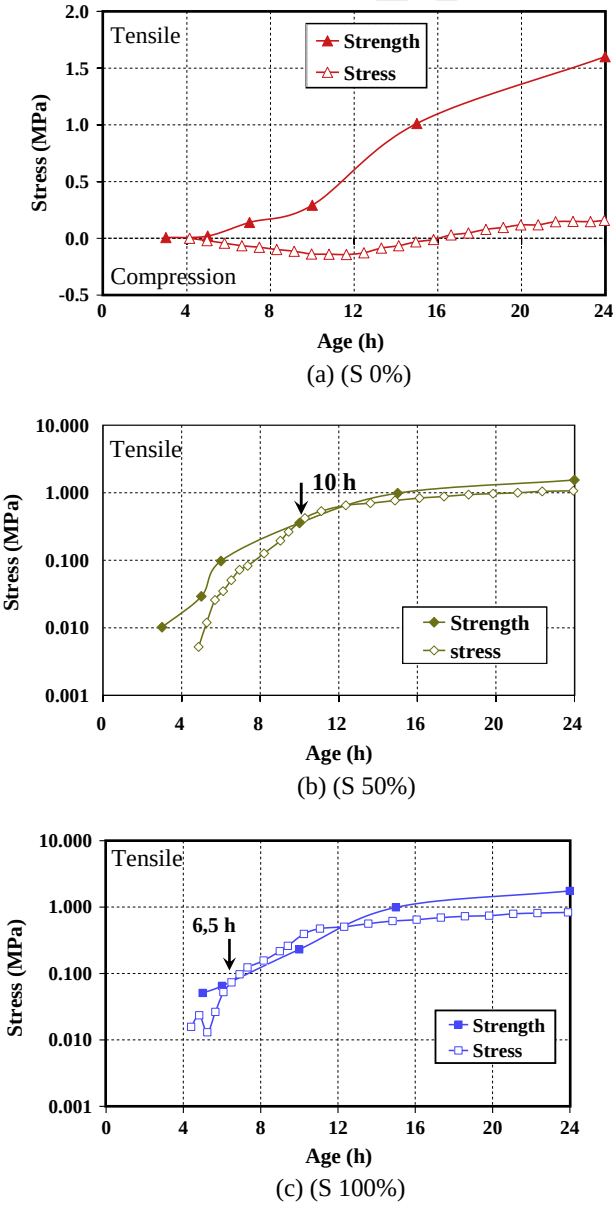

Fig. 11. Evolution of the predicted internal stresses due to autogenous shrinkage and the experimental values of the tensile strength.

The comparison presented in Fig. 11 shows that the internal stresses due to total restraint of autogenous shrinkage would remain much lower than the tensile strength of concrete (S 0%),

thus the potential risk of cracking was relatively low. This comes from the early age swelling due to higher bleeding. As shown in Fig. 11, internal stresses due to autogenous shrinkage are likely to become higher than the tensile strength of (S 50%) and (S 100%) at early age. (S 100%) was characterised by the highest stresses development before 8 h. This shows the prevailing influ ence of the rapid increase of the elastic modulus during the first hours, whereas the tensile strength remained relatively low. As a consequence, the potential risk of cracking by restrained autoge nous shrinkage of these formulations was high relatively to strength at this age. (S 0%) remained the safest concrete compara bly to (S 50%) and (S 100%), dealing with the potential risk of cracking by restrained autogenous shrinkage. This effect of the (Added water/Cement) ratio is consistent with an experimental study on the effect of the (Water/Cement) ratio on the stress gen eration due to restrained shrinkage [9]; the stress increases with a decrease in (Water/Cement) ratio.

It is important to note that such results do not take into account the creep and relaxation phenomena of the concrete and any cou pling between shrinkage and strength development. The creep strain develops rapidly at very early age thus stress relaxation due to creep can overcome the rapidly increasing shrinkage in duced tensile stress. As the three concretes were made of the same raw materials and derived from the same reference mixture, the (Added water/Cement) ratio mainly influences creep and relaxa tion. Experimental studies have shown that creep increases with (Water/Cement) ratio [44,45]. Moreover model codes such as CEB FIP Model Code 1990 [46] often consider that creep increases with a decrease in compressive strength. As a consequence con crete (S 0%) would benefit from the highest relaxation and show the lowest risk of cracking due to restrained shrinkage.

5. Conclusions

In this paper, a comprehensive set of experimental data about the effect of the initial water saturation of limestone aggregates on shrinkage is presented. The experimental study deals with early age cracking. Assuming that good curing practice has been done, the paper is focused on the causes and consequences of autogenous shrinkage. The investigation was carried out at macro scopic and microscopic scale. An estimation of the relative risk of cracking risk due to restrained autogenous shrinkage was also proposed based on the evolution of the elastic properties and the autogenous shrinkage evolution at early age. The main conclusions of this study can be summarized as follows:

The concept of the effective water is overly simplified when using aggregates with significant water absorption. The effec tive water consists in adjusting the added water to take into account the absorption of mixing water into porous aggregate that has been batched dry or at moisture content less than its absorption, in order to keep the total water constant. Three con crete mixtures were derived from a reference concrete mixture by varying only the initial water saturation of gravel, namely: dry, partially saturated and totally saturated. This results in concretes with significantly different behaviour. The actual amount of water absorbed by dry or partially saturated aggre gates can be different from the theoretical amount, which is based on absorption capacity of the aggregates. The behaviour of concrete is strongly related to the (Added water/Cement) ratio, which depends on the aggregates initial degree of satura tion for given effective water content.

Concrete made of partially saturated aggregates (S 50%) did not have intermediate behaviour between concrete made of dry aggregates (S 0%) and saturated aggregates (S 100%). It showed the highest autogenous and plastic shrinkage at early age, and the highest compressive strength. (S 50%) contained less added water than (S 0%) and did not take advantage of the internal curing by saturated aggregates as (S 100%).

The investigation carried out at the macroscopic scale can bring interesting information about the microstructure to understand the effect of the water saturation of aggregates. As suggested by the values of strength and porosimetry mesurements, the initial water content of aggregates is likely to influence the porosity distribution of the cement paste. Initially dry aggregates (S 0%) resulted in higher macroporosity and lower strength. Concrete made of saturated aggregates (S 100%) showed higher mesoporosity and lower strength than partially saturated aggregates (S 50%).

The methodology to assess the relative cracking risk was based on the stress/strength evaluation and experimental parameters. Stresses were calculated using autogenous shrinkage and elastic modulus data. The strength of early age concrete was obtained from direct tensile testing. The concrete with initially saturated aggregates showed the highest potential risk of cracking, because of the rapid evolution of elastic modulus from initial setting time.

Acknowledgements

This work was supported by the *Fédération Nationale des Travaux Publics*, FNTP (French National Association of Contractors). The authors gratefully acknowledge material supplied by UNPG (National Association of Aggregate Producers). This research is partially financed by grants funded by the Belgian National Foundation for Scientific Research (FRFC), which is gratefully acknowledged.

References

[1] Fujiwara T. Effect of aggregate on drying shrinkage of concrete. J Adv Concr Tech 2008;6(1):31–44.
[2] Ollivier J-P, Maso J-C, Bourdette B. Interfacial transition zone in concrete. Adv Cem Bas Mater 1995;2(1):30–8.
[3] Verbeck G, Landgren R. Influence of physical characteristics of aggregates on frost resistance of concrete. ASTM, Philadelphia 1960;3(60):1063–79.
[4] Bisschop J, Van Mier JGM. Effect of aggregates on drying shrinkage microcracking in cement-based composites. Mater struct 2002;35(8):453–61.
[5] Zhutovsky S, Kovler K, Bentur A. Efficiency of lightweight aggregates for internal curing of high strength concrete to eliminate autogenous shrinkage. Mater Struct 2002;35:97–101.
[6] Bentz DP, Snyder KA. Protected paste volume in concrete extension to internal curing using saturated lightweight fine aggregate. Cem Concr Res 1999;29:1863–7.
[7] Lura P. Internal water curing with Liapor aggregates. HERON 2005;50:1.
[8] Henkensiefken R, Bentz D, Nantung T, Weiss J. Volume change and cracking in internally cured mixtures made with saturated lightweight aggregate under sealed and unsealed conditions. Cem Concr Compos 2009;31:427–37.
[9] Toma G, Comportement des bétons au jeune âge, PhD Thesis, Canada: University of Laval; 1999.
[10] Alhozaimy AM. Effect of absorption of limestone aggregates on strength and slump loss of concrete. Cem Concr Compos 2009;31:470–3.
[11] Pereira CG, Castro-Gomes J, Pereira de Oliveira L. Influence of natural coarse aggregates size, mineralogy and water content on the permeability of structural concrete. Constr Build Mater 2009;23:602–8.
[12] Elsharief A, Cohen MD, Olek J. Influence of lightweight aggregate on the microstructure and durability of mortar. Cem Concr Res 2005;35:1368–76.
[13] Ayhan M, Gönül H, Gönül I, Karakus A. Effect of basic pumice on morphologic properties of interfacial transition zone in load-bearing lightweight/semi-lightweight concretes. Constr Build Mater 2011;25:2507–18.
[14] Courard L, Lenaers J-F, Michel F, Garbacz A. Saturation level of the superficial zone of concrete and adhesion of repair systems. Constr Build Mater 2011;25:2488–94.
[15] Mallat A, Alliche A. Mechanical investigations of two repair mortars and repaired system, Actes de la 29ème Rencontre de l'AUGC, 29–31 mai 2011, Tlemcen, vol. I – Génie de la construction, p. 355.
[16] BS EN 1097-6, Tests for mechanical and physical properties of aggregates. Determination of particle density and water absorption; June 2001.

Accepted Manuscript

[17] Turcry P, Loukili A. Evaluation of plastic shrinkage cracking of self-consolidating concrete. ACI Mater J 2006;103(4):272–9.
[18] Saliba J, Rozière E, Grondin F, Loukili A. Influence of shrinkage-reducing admixtures on plastic and long-term shrinkage. Cem Concr Compos 2011;33:209–17.
[19] EN 196-3. Methods of testing cement – Part 3: determination of setting times and soundness; 2005.
[20] BTJADE. Equipment for the determination of autogenous shrinkage of concrete at early age. <http://www.lcpc.fr/francais/produits/materiels-mlpc-r/fiche-mlpc-r/article/btjade>.
[21] Boulay C. Test rig for early age measurements of the autogenous shrinkage of a concrete, CONCRACK3 – RILEM-JCI international workshop on crack control of mass concrete and related issues concerning early-age of concrete structures, 15–16 March 2012, Paris, France.
[22] Boulay C, Patiès C. Mesure des déformations du béton au jeune âge. Mater Struct 1993;26:307–11.
[23] Staquet S, Boulay C, Robeyst N, De Belie N. Ultrasonic monitoring of setting and autogenous shrinkage development of high performance concrete, creep, shrinkage and durability mechanics of concrete and concrete structures, Tanabe et al. editor. In: proceedingc. of the 8th international conference on creep, shrinkage and durability of concrete and concrete structures (CONCREEP 8), 321–327.
[24] Laplante P, Boulay C. Evolution du coefficient de dilatation thermique du béton en fonction de sa maturité aux tout premiers âges. Mater struct 1994;27:596–605.
[25] Reinhardt HW, Grosse CU. Continuous monitoring of setting and hardening of mortar and concrete. Constr Build Mater 2004;18:145–54.
[26] Kurz JH, Grosse CU, Reinhardt HW. Strategies for reliable automatic onset time picking of acoustic emissions and of ultrasound signals in concrete. Ultrasonics 2005;43:538–46.
[27] Krauß M, Hariri K. Determination of initial degree of hydration for improvement of early-age properties of concrete using ultrasonic wave propagation. Cem Concr Compos 2006;28:299–306.
[28] Diamond S. Review – Mercury porosimetry, an inappropriate method for the measurement of pore size distributions in cement-based materials. Cem Concr Res 2000;30:1517–25.
[29] Loukili A, Khelidj A, Richard P. Hydration kinetics, change of relative humidity, and autogenous shrinkage of ultra-high-strength concrete'. Cem Concr Res 1999;29:577–84.
[30] Bogue RH. Calculation of the compounds in Portland cement. Indust Eng Chem Anal Ed 1929;1:192–7.
[31] Roziere E, Cortas R, Loukili A. How to investigate the tensile behaviour of early age concrete? Amsterdam: Microdurability; April 2012. p. 11–13.
[32] Almusallam AA, Maslehuddin M, Abdul-Waris M, Khan MM. Effect of mix propotions on plastic shrinkage cracking of concrete in hot environments. Constr Build Mater 1998;12:353–8.
[33] Darquennes A. Comportement au jeune âge de bétons formulés à base de ciment au laitier de haut fourneau en condition de déformations libre et restreinte, PhD thesis. Université Libre de Bruxelles; 2009.
[34] Bjøntegaard Ø, Thermal dilation and autogenous deformation as driving forces to self-induced stresses in high performance concrete, Dr.ing. theses 1, Trondheim: The Norwegian University of Science and Technology; 1999. p. 121.
[35] Hammer TA, Bjøntegaard Ø, Sellevold EJ. Measurement methods for testing of early age autogenous strain. In: Early age cracking in cementitious systems. Cachan: RILEM TC 181-EAS Committee, RILEM; 2002. p. 207–15.
[36] Josserand L, Coussy O, de Larrard F. Bleeding of concrete as an ageing consolidation process. Cem Concr Res 2006;36:1603–8.
[37] Verbeck GJ, Helmuth RH. Structures and physical properties of hardened cement paste. In: 5th International Symposium On The Chemistry Of Cement, Tokyo, 3(7–1) 1968, p. 1–11.
[38] Diamond S. Cement paste microstructure: an overview at several levels. In: Proceeding. of the conference of Sheffield on hydraulic cement pastes, vol. 8–9, Cement and Concrete Association; April 1976.
[39] Scrivener K, Alison K, Laugesen C et P. The interfacial transition zone (ITZ) Between Cement Paste and Aggregate in concrete. Interf Sci 2004;12:411–21.
[40] Bjøntegaard Ø. Thermal dilation and autogenous deformation as driving forces to self-induced stresses in high performance concrete. PhD thesis. Norway: NTNU; 1999. p. 256.
[41] Hammer TA, Fossa KT, Bjøntegaard Ø. Cracking tendency of HSC: tensile strength and self generated stress in the period of setting and early hardening. Mater struct 2007;40:319–24.
[42] Darquennes A, Staquet S, Delplancke-Ogletree M-P, Espion B. Effect of autogenous deformation on the cracking risk of slag cement concretes. Cem Concr Compos 2011;33:368–79.
[43] Ravina D, Shalon R. Plastic shrinkage cracking. ACI J 1968;65(22):282–94.
[44] Domone PL. Uniaxial tensile creep and failure of concrete. Mag Concr Res 1974;26(88):144–52.
[45] Lee Y, Yi S-T, Kim M-S, Kim J-K. Evaluation of a basic creep model with respect to autogenous shrinkage. Cem Concr Res 2006;36:1268–78.
[46] CEB-FIP, editor. Model code 1990 – design code. London: Thomas Telford; 1993.

Accepted Manuscript